Inorganic Chemistry

Article

pubs.acs.org/IC

Periodic Trends in Hexanuclear Actinide Clusters

Juan Diwu, Shuao Wang, and Thomas E. Albrecht-Schmitt*

Department of Civil Engineering and Geological Sciences and Department of Chemistry and Biochemistry, University of Notre Dame, Notre Dame, Indiana 46556, United States

Supporting Information

ABSTRACT: Four new Th(IV), U(IV), and Np(IV) hexanuclear clusters with 1,2-phenylenediphosphonate as the bridging ligand have been prepared by self-assembly at room temperature. The structures of $Th_6Tl_3[C_6H_4(PO_3)(PO_3H)]_6(NO_3)_7(H_2O)_6{\cdot}(NO_3)_2{\cdot}4H_2O$ (**Th6-3**), $(NH_4)_{8.11}Np_{12}Rb_{3.89}[C_6H_4(PO_3)(PO_3H)]_{12}(NO_3)_{24}{\cdot}15H_2O$ (**Np6-1**), $(NH_4)_4U_{12}Cs_8[C_6H_4(PO_3)(PO_3H)]_{12}(NO_3)_{24}{\cdot}18H_2O$ (**U6-1**), and $(NH_4)_4U_{12}Cs_2[C_6H_4(PO_3)(PO_3H)]_{12}(NO_3)_{18}{\cdot}40H_2O$ (**U6-2**) are described and compared with other clusters of containing An(IV) or Ce(IV). All of the clusters share the common formula $M_6(H_2O)_m[C_6H_3(PO_3)(PO_3H)]_6(NO_3)_n^{(6-n)}$ (M = Ce, Th, U, Np, Pu). The metal centers are normally nine-coordinate, with five oxygen atoms from the ligand and an additional four either occupied by NO_3^- or H_2O. It was found that the Ce, U, and Pu clusters favor both C_{3i} and C_i point groups, while Th only yields in C_i, and Np only C_{3i}. In the C_{3i} clusters, there are two NO_3^- anions bonded to the metal centers. In the C_i clusters, the number of NO_3^- anions varies from 0 to 2. The change in the ionic radius of the actinide ions tunes the cavity size of the clusters. The thorium clusters were found to accept larger ions including Cs^+ and Tl^+, whereas with uranium and later elements, only NH_4^+ and/or Rb^+ reside in the center of the clusters.

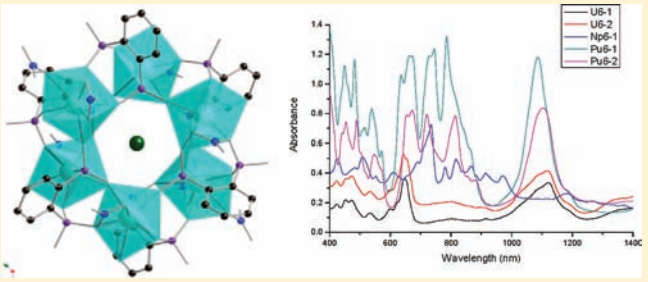

INTRODUCTION

Actinide cluster chemistry is poorly developed when compared to that of transition metals or lanthanides.[1] The most explored system is that of actinyl peroxides, which have yielded a vast array of unusual topologies.[2] The largest cluster reported thus far contains 60 uranium centers and adopts a fullerene topology.[2e] A single peroxide cluster has been reported with neptunium, and the evidence suggests it is mixed-valent and contains both Np(V) and Np(VI).[3] Attempts to prepare plutonium peroxide clusters instead yielded the first examples of crystallized forms of the so-called plutonium colloid, which in actuality is nanocrystals of plutonium oxide with the fluorite structure where the exterior of the cluster is passivated with chloride. The number the plutonium centers in these clusters can vary, and the first reported one is a Pu_{38} cluster.[4] Clusters of tetravalent actinides are expected to be more difficult to prepare than those with higher oxidation states owing the remarkable insolubility and high susceptibility to hydrolysis of +4 actinide cations. Tetravalent metal clusters are well-known, especially with Zr(IV) and Ce(IV).[5] For example, hexanuclear Ce(IV) carboxylates were reported to be able to oxidize certain organic compounds.[5h] Ce(IV)/Ln(III) clusters show strong luminescence that is both metal- and ligand-based.[5i] Tetravalent uranium oxo/hydroxo clusters of U_6, U_{10}, and U_{16} are established.[6] Hexanuclear thorium clusters with carboxylate ligands were recently reported by Takao et al. and Soderholm et al.[6b,7] In almost all of the aforementioned clusters, the metal centers are linked to one another by an oxo bridge, which limits the cavity size of the clusters.

We recently communicated the successful isolation of Ce(IV), Th(IV), and Pu(IV) hexanuclear clusters.[8] Herein we substantially expand this work with further examples of Th(IV) clusters as well as those with U(IV) and Np(IV), thus completing the early actinide series with metals that have stable +4 oxidation states in water. Four new clusters are reported: $Th_6Tl_3[C_6H_4(PO_3)(PO_3H)]_6(NO_3)_7(H_2O)_6{\cdot}(NO_3)_2{\cdot}4H_2O$ (**Th6-3**), $(NH_4)_{8.11}Np_{12}Rb_{3.89}[C_6H_4(PO_3)(PO_3H)]_{12}(NO_3)_{24}{\cdot}15H_2O$ (**Np6-1**), $(NH_4)_4U_{12}Cs_8[C_6H_4(PO_3)(PO_3H)]_{12}(NO_3)_{24}{\cdot}18H_2O$ (**U6-1**), and $(NH_4)_4U_{12}Cs_2[C_6H_4(PO_3)(PO_3H)]_{12}(NO_3)_{18}{\cdot}40H_2O$ (**U6-2**). These clusters are compared with the previous members of the series. Using these six clusters, we demonstrate that the cavity size of the cluster is tuned by the ionic radius of the cations and that the clusters only assemble around monovalent cations of specific size. We also explore the coordination chemistry of the tetravalent actinides and changes in the symmetry of the clusters.

EXPERIMENTAL SECTION

Syntheses. $^{237}NpO_2$ (99.9%, Oak Ridge, $t_{1/2} = 2.14 \times 10^6$ y) *also represents a serious health risk owing to its α and γ emission.* Specialized facilities and procedures are needed for this work. All free-flowing solids are worked with in negative-pressure gloveboxes, and products are only examined when coated with either water or Krytox oil and water. There are some limitations in accurately determining yield with neptunium and plutonium compounds because this requires weighing

Received: October 30, 2011
Published: March 21, 2012

dx.doi.org/10.1021/ic2023242 | Inorg. Chem. 2012, 51, 4088–4093

a dry solid, which poses certain risks as well as manipulation difficulties given the small quantities that we work with. UCl_4 (99%, international bioanalytical industries) was used as received.

*$Th_6Tl_3[C_6H_4(PO_3)(PO_3H)]_6(NO_3)_7(H_2O)_6{\cdot}(NO_3)_2{\cdot}4H_2O$ (**Th6-3**).* **Th6-3** crystals were obtained by mixing $Th(NO_3)_4$ solution (0.1 M, 0.9 mL), 1,2-phenylenediphosphonic acid (0.1 M, 0.1 mL), $TlNO_3$ (0.1 M, 0.6 mL) together into a 4 mL scintillation vial, followed by slow evaporation at room temperature. The colorless block crystals of **Th6-3** were observed after 1 week.

*$(NH_4)_{8.11}Np_{12}Rb_{3.89}[C_6H_4(PO_3)(PO_3H)]_{12}(NO_3)_{24}{\cdot}15H_2O$ (**Np6-1**).* Crystals of **Np6-1** were synthesized by mixing a $NpO_2(NO_3)$ solution (5.3 mg of NpO_2OH dissolved in 100 μL of concentrated HNO_3), $N_2H_4{\cdot}2HCl$ solution (2 M, 44 μL), RbOH (0.1 M, 100 μL), CsOH (0.1 M, 100 μL), 1,2-phenylenediphosphonic acid (0.1 M, 0.1 mL) in a 4 mL vial, followed by slow evaporation at room temperature for several weeks. The pale yellow-green trigonal crystals of **Np6−1** formed on the bottom of the vial.

*$(NH_4)_4U_{12}Cs_8[C_6H_4(PO_3)(PO_3H)]_{12}(NO_3)_{24}{\cdot}18H_2O$ (**U6-1**) and $(NH_4)_4U_{12}Cs_2[C_6H_4(PO_3)(PO_3H)]_{12}(NO_3)_{18}{\cdot}40H_2O$ (**U6-2**).* Both **U6-1** and **U6-2** crystals were isolated from the same reaction. UCl_4 (4.8 mg), $N_2H_4{\cdot}2HCl$ solution (2 M, 100 μL), RbOH (0.1 M, 100 μL), CsOH (0.1 M, 100 μL), HNO_3 (0.1 M, 100 μL), and 1,2-phenylenediphosphonic acid (0.1 M, 0.1 mL), were mixed in a 4 mL vial and allowed to evaporate at room temperature for 2 days. Green crystals of **U6-1** (trigonal) and **U6-2** (block) were isolated.

Note: We were able to conduct many reactions on Ce and Th to explore the combinatorial parameters of pH, cation, and reaction stoichiometry for assembling these clusters, but only found two structure types, C_{3i} and C_i. Owing to the difficulties in manipulating U^{4+} and Np^{4+} reactions, we were only able to start two or three such reactions. For example, Np reactions were conducted with only 5 mg of NpO_2 each, but we need enough time for it to crystallize out, so the total volume is increased for longer evaporation times. Short evaporation time will only yield amorphous powders. For U^{4+}, longer evaporation time will result in U^{6+} products, because U^{4+} is easily oxidized by oxygen in air. For this reason, we reduced the total volume to allow the U^{4+} crystals to grow in just 2 days. The fact that these clusters can form under such diverse conditions supports that they are the only preferred cluster forms.

Crystallographic Studies. All crystals were mounted on CryoLoops with Krytox oil and optically aligned on a Bruker APEXII Quazar X-ray diffractometer using a digital camera. Initial intensity measurements were performed using an IμS X-ray source, a 30 W microfocused sealed tube (MoKα, λ = 0.71073 Å) with high-brilliance and high-performance focusing Quazar multilayer optics. For all the data sets, standard APEXII software was used for determination of the unit cells and data collection control. The intensities of reflections of a sphere were collected by a combination of four sets of exposures (frames). Each set had a different φ angle for the crystal and each exposure covered a range of 0.5° in ω. A total of 1464 frames were collected with an exposure time per frame of 10−80 s, depending on the crystal. SAINT software was used for data integration including Lorentz and polarization corrections. Semiempirical absorption corrections were applied using the program SCALE (SADABS).[9] In all of the structure models, all of the atoms are refined anisotropically. Level A alerts resulting from having isolated water molecules exist in all the cifchecks, because those water molecules are highly disordered that no hydrogen atoms could be located. The protons of the benzene rings were placed in fixed, calculated positions in all the compounds. Selected crystallographic information is listed in Table 1. Further details of the crystal structure investigation may be obtained from the crystal structure database on quoting numbers CSD 848002−848005.

UV−vis-NIR Spectroscopy. UV−vis-NIR data were acquired from single crystals using a Craic Technologies microspectrophotometer. Crystals were placed on quartz slides under Krytox oil, and the data were collected from 400 to 1400 nm.

Table 1. Crystallographic Data for $Th_6Tl_3[C_6H_4(PO_3)(PO_3H)]_6(NO_3)_7(H_2O)_6{\cdot}(NO_3)_2{\cdot}4H_2O$ (Th6-3), $(NH_4)_{8.11}Np_{12}Rb_{3.89}[C_6H_4(PO_3)(PO_3H)]_{12}(NO_3)_{24}{\cdot}15H_2O$ (Np6-1), $(NH_4)_4U_{12}Cs_8[C_6H_4(PO_3)(PO_3H)]_{12}(NO_3)_{24}{\cdot}18H_2O$ (U6-1), and $(NH_4)_4U_{12}Cs_2[C_6H_4(PO_3)(PO_3H)]_{12}(NO_3)_{18}{\cdot}40H_2O$ (U6-2)

compound	Th6-3	Np6-1	U6-1	U6-2
formula mass	4375.44	3889.17	4251.98	3911.20
color and habit	colorless, block	pale-yellow-green, hexagon plate	green, hexagon-plate	green, block
space group	$P\bar{1}$ (No. 2)	$R\bar{3}$ (No. 148)	$R\bar{3}$ (No. 148)	$P\bar{1}$ (No. 2)
a (Å)	12.192(2)	17.1998(7)	17.253(3)	17.06(1)
b (Å)	15.644(2)	17.1998(7)	17.253(3)	17.11(1)
c (Å)	16.615(2)	17.1998(7)	17.253(3)	18.69(1)
α (deg)	112.696(1)	97.1400(1)	97.550(1)	96.47(1)
β (deg)	108.561(2)	97.1400(1)	97.550(1)	100.38(2)
γ (deg)	98.826(2)	97.1400(1)	97.550(1)	103.75(1)
V (Å^3)	2629.5(6)	4959.1(3)	4989.1(13)	5142(7)
Z	1	1	2	1
T (K)	100(2)	100(2)	100(2)	100(2)
λ (Å)	0.71073	0.71073	0.71073	0.71073
maximum 2θ (deg)	27.56	27.51	27.50	27.47
ρ_{calcd} (g cm^{-3})	2.763	2.605	2.830	2.526
μ(Mo $K\alpha$) (cm^{-1})	133.39	75.00	114.63	100.80
$R(F)$ for $F_o^2 > 2\sigma(F_o^2)^a$	0.0415	0.0372	0.0501	0.0540
$R_w(F_o^2)^b$	0.0870	0.1120	0.1417	0.1324

$^aR(F) = \sum||F_o| - |F_c||/\sum|F_o|$. $^bR_w(F_o^2) = [\sum[w(F_o^2 - F_c^2)^2]/\sum wF_o^4]^{1/2}$.

RESULTS AND DISCUSSION

Synthesis. In order to ascertain all of the parameters for assembling hexanuclear clusters, a combinatorial approach was taken where the effects of pH, counterions, and the stoichiometry of the reactants was varied. We demonstrated that the most important feature is the size of the counterions that the clusters assemble around. These clusters only form with cations of specific sizes. Even though pH and stoichiometry also affected the yield, the range for the formation of such clusters is quite wide.

Since both thorium and plutonium are able to form this type of cluster, based on the ionic radius similarities, uranium and neptunium, in their tetravalent states, should be able to form the same type of cluster. However, the most obvious problem we encountered was how to achieve and maintain a tetravalent state in the presence of oxygen. Thorium almost exclusively exists as tetravalent cations. For plutonium, on the other hand, even though it can exist in +3, +4, +5, and +6 oxidation states, its most stable state in the presence of oxygen is Pu(IV).[10] The use of excess nitrite as a reducing agent allowed us to easily access Pu(IV). Uranium and neptunium are both able to adopt +4 oxidation states, but both are somewhat air-sensitive. The use of excess hydrazine allowed us to stabilize U(IV) and Np(IV) long enough to crystallize the clusters. We were able to isolate crystals of $(NH_4)_{8.11}Rb_{3.89}Np_{12}[C_6H_4(PO_3)(PO_3H)]_{12}(NO_3)_{24}15H_2O$ (**Np6-1**), $(NH_4)_4Cs_8U_{12}$ $[C_6H_4(PO_3)(PO_3H)]_{12}(NO_3)_{24}{\cdot}18H_2O$ (**U6-1**), and $(NH_4)_4Cs_2U_{12}$ $[C_6H_4(PO_3)(PO_3H)]_{12}(NO_3)_{18}{\cdot}40H_2O$ (**U6-2**) in high yield. Thorium clusters only crystallize

dx.doi.org/10.1021/ic2023242 | Inorg. Chem. 2012, 51, 4088−4093

with the large cations Cs^+ and Tl^+. For uranium and neptunium reactions, both Rb^+ and Cs^+ were tested. However, the hydrazine in the reactions creates a complication in that once it is oxidized it becomes NH_4^+, which has almost the same ionic radius as Rb^+ (148 pm), and these cations disorder within the structures.

Structure Descriptions. The ligand 1,2-phenylenediphosphonate (**PhP2**) both chelates and bridges between the metal centers. In all compounds, the ligand is partially deprotonated and is described as $[C_6H_4(PO_3)(PO_3H)]^{3-}$ (based on bond distances and bond-valence sum calculations). The PO_3 moiety is bonded to three metal centers, while the PO_3H group only bonds to two metal centers and has one protonated oxo atom. A total of six diphosphonate ligands serve to bridge between the six metal centers, and the clusters can be generally catagorized as M_6L_6 clusters.

The metal centers are chelated by four PO_3 groups from two **PhP2** ligands. The remaining donor oxygen atoms that coordinate the metal centers are from either NO_3^- or H_2O. The clusters are all anionic with a single cation trapped within the cage and several others residing between the clusters.

Structure of $Th_6Tl_3[C_6H_4(PO_3)(PO_3H)]_6(NO_3)_7(H_2O)_6 \cdot (NO_3)_2(H_2O)_4$ (Th6-3). The **Th6-3** is very similar to the previously reported **Th6-1** and **Th6-2** clusters. **Th6-3** crystallizes in triclinic space group $P\bar{1}$. There are three unique thorium centers in the structure, all are nine-coordinate, tricapped trigonal prisms. However, Th1 and Th2 only bond to one NO_3^- anion and two H_2O molecules, while Th3 is bound by one NO_3^- anion, one H_2O molecule, and it shares one NO_3^- anion with another Th3 center from an adjacent cluster. Tl^+ cations reside in the cavity in the center of the cluster. The previously reported thorium clusters all have Cs^+ as the counterion. Figure 1 shows the topology of this thorium cluster,

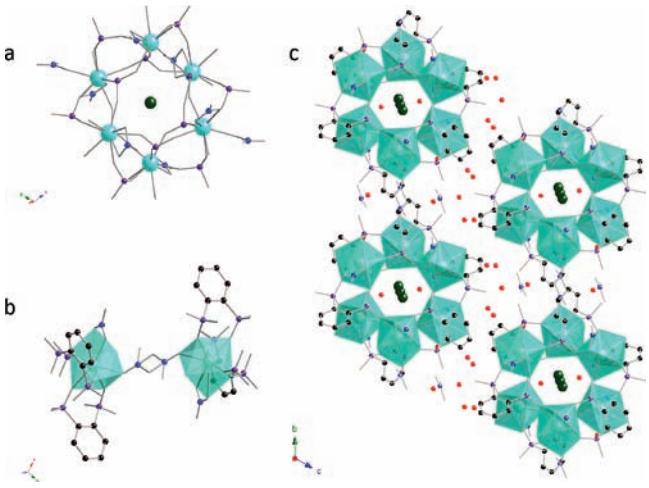

Figure 1. Illustration of the $Th_6Tl_3[C_6H_4(PO_3)(PO_3H)]_6(NO_3)_7(H_2O)_6 \cdot (NO_3)_2(H_2O)_4$ (**Th6-3**) cluster. (a) The cluster topology showing the Th6 core and the coordination environment of the thorium; benzene rings are removed for clarity; (b) the detailed depiction of the disordered NO_3^- between two thorium centers; (c) the arrangement of the thorium clusters and the free water molecules, Tl^+ and NO_3^- positions between the clusters. Color code: light blue: Th; dark blue: N; dark green: Rb; purple: P; red: O.

especially the disordered NO_3^- in Figure 1b. Figure 1c is the packing of the thorium clusters with free water molecules and Tl^+ cations residing between the clusters. The ionic radius of Tl^+ (164 pm) is very close to that of Cs^+ (169 pm). Attempts to incorporate smaller cations such as Rb^+ and K^+ failed to yield crystalline products.

$Np_{12}Rb_{3.89}[C_6H_4(PO_3)(PO_3H)]_{12}(NH_4)_{8.11}(NO_3)_{24} \cdot (H_2O)_{15}$ (Np6-1). **Np6-1** crystallizes in the rhombohedral space group $R\bar{3}$. In one asymmetric unit, there are two unique Np centers. However, their coordination environments are almost identical. Each of the two neptunium sites generates one hexanuclear cluster by the C_{3i} symmetry operation. The Np(IV) cations are found as nine-coordinate, tricapped trigonal prisms. Among the nine oxygen atoms that are bonded to the neptunium centers, four of them are from chelating nitrate, and five are from the **PhP2** ligands. The topology of the clusters is shown in Figure 2a;

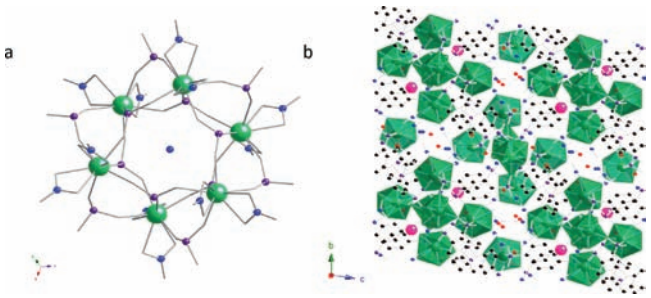

Figure 2. Illustration of the $Np_{12}Rb_{3.89}[C_6H_4(PO_3)(PO_3H)]_{12}(NH_4)_{8.11}(NO_3)_{24} \cdot (H_2O)_{15}$ (**Np6-1**) cluster. (a) The cluster topology showing the Np6 core and the coordination environment of the Np; benzene rings are removed for clarity; (b) the arrangement of the neptunium clusters and the free water and Rb^+ positions between the clusters. Color code: light green: Np; dark blue: N; pink: Cs; purple: P; red: O.

carbon atoms are removed for clarity. The cavity of the clusters are occupied by the NH_4^+ cations which reside on $\bar{3}$ sites. There are also Rb^+ cations in the structure disordered with the NH_4^+ cations. The packing arrangement of the clusters is shown in Figure 2b.

$U_{12}Cs_8[C_6H_4(PO_3)(PO_3H)]_{12}(NO_3)_{24} \cdot (NH_4)_4(H_2O)_{18}$ (U6-1). **U6-1** also crystallized in $R\bar{3}$. There are two unique uranium centers; both have the same coordination environment and generate one hexanuclear cluster. Two NO_3^- anions chelate the metal centers as shown in Figure 3a. In **U6-1**, the NH_4^+ cations

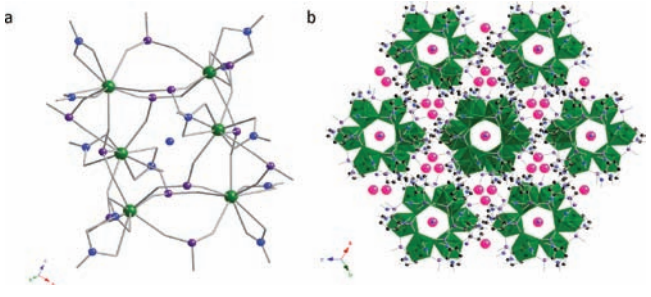

Figure 3. Illustration of the $U_{12}Cs_8[C_6H_4(PO_3)(PO_3H)]_{12}(NO_3)_{24} \cdot (NH_4)_4(H_2O)_{18}$ (**U6-1**) cluster. (a) The cluster topology showing the U6 core and the coordination environment of the U; benzene rings are removed for clarity; (b) the arrangement of the uranium clusters and the free water and Cs^+ positions between the clusters. Color code: green: U; dark blue: N; pink: Cs; purple: P; red: O.

reside in the cavity of the cluster; however, it was also found that Cs^+ cations were between the clusters. Curiously, even

dx.doi.org/10.1021/ic2023242 | Inorg. Chem. 2012, 51, 4088–4093

when Rb^+ added to the reactions, it is not found within the crystals. The arrangement of the clusters is the same as in the Np(IV) clusters and is shown in Figure 3b.

$U_{12}Cs_2[C_6H_4(PO_3)(PO_3H)]_{12}(NO_3)_{18}\cdot(NH_4)_4(H_2O)_{40}$ (U6-2). This uranium cluster crystallizes in the $P\bar{1}$ space group; however, the unit cell is much larger than all the other triclinic clusters because there are six different uranium centers in one asymmetric unit. In other triclinic clusters, there are only three unique metal centers. On the basis of the C_i symmetry operation, these metal centers generate one cluster. However, in **U6-2**, there are two types of clusters, differing in the number of NO_3^- anions. U1, U2, and U3 from one cluster have 2, 2, and 1 NO_3^- anions in the coordination sphere, respectively. U4, U5, and U6 from the second cluster have 2, 1, and 1 NO_3^- each. Although there are two NO_3^- anions bonded to U4, they are disordered and are half-occupied. The counterion that resides inside the clusters is solely NH_4^+, while both NH_4^+ and Cs^+ exist between clusters.

COMPARISONS OF CLUSTERS

Ten diffferent hexanuclear clusters have been prepared with tetravalent actinides or Ce(IV): three with thorium (**Th6-1**, **Th6-2**, and **Th6-3**), two with uranium (**U6-1** and **U6-2**), one with neptunium (**Np6-1**), and two with plutonium (**Pu6-1** and **Pu6-2**), and two with cerium (**Ce6-1** and **Ce6-2**).[8] These clusters are compared in Table 2.

Table 2. Comparison of Hexanuclear An(IV) and Ce(IV) Clusters

	Th	U	Np	Pu/Ce
point group	C_i	C_{3i}, C_i	C_{3i}	C_{3i}, C_i
coordination number	8, 9	9	9	9
counterion inside	Cs^+, Tl^+	NH_4^+	Rb^+, NH_4^+	NH_4^+
counterion outside	Cs^+, Tl^+	Cs^+, NH_4^+	Rb^+, NH_4^+	NH_4^+
NO_3^- no.	0, 1, 1.5, 2	1, 2	2	2
free NO_3^-	yes	no	no	no
distance to center of cluster (Å)	4.510 (Cs^+) 4.566 (Tl^+)	4.430	4.416	4.405 (Pu) 4.414 (Ce)

The possible point groups for the clusters are C_{3i} and C_i. Two types of clusters normally crystallize from the same reaction with uranium, plutonium, and cerium. However, not all the elements can adopt both space groups at the same time. Thorium was only found in the C_i system, although there were three different unit cells. In contrast, Np(IV) cluesters were only found with the C_{3i} point group.

The most common coordination environment in these clusters is a nine-coordinate tricapped trigonal prism. However, counterintuitively there is one thorium center in **Th6-2** that is eight-coordinate. Calculations demonstrate that the geometry for this ThO_8 unit is best described as a D_{4d} square antiprism.[11] Comparisons of the M−O (M = Ce, Th, U, Np, Pu) bond distances clearly demonstrate the actinide contraction. For the C_{3i} clusters, the average bond distances are **U6-1** (2.428 Å) > **Np6-1** (2.407 Å) > **Ce6-1** (2.401 Å) ~ **Pu6−1** (2.400 Å). The C_i clusters show the same trend: Th6−1 (2.471 Å) (only two nine-coordinate sites were used) ~ **Th6−3** (2.467 Å) ~ **Th6−2** (2.462 Å) > **U6-2** (2.423 Å) > **Ce6-2** (2.395 Å) ~ **Pu6-2** (2.391 Å).

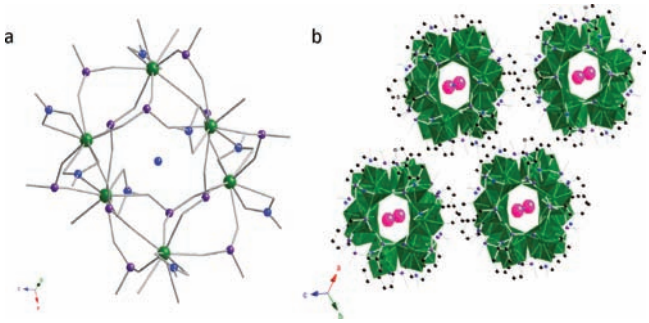

Figure 4. Illustration of the $U_{12}Cs_2[C_6H_4(PO_3)(PO_3H)]_{12}(NO_3)_{18}\cdot(NH_4)_4(H_2O)_{40}$ (**U6-2**) cluster. (a) The cluster topology showing the U6 core and the coordination environment of the U; benzene rings are removed for clarity; (b) the arrangement of the uranium clusters, and the free water and Cs^+ positions between the clusters. Color code: green: U; dark blue: N; pink: Cs; purple: P; red: O.

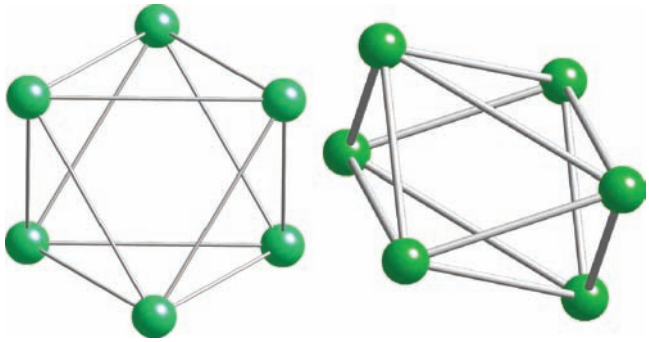

Figure 5. Views of the C_{3i} (left) (**Ce6-1**, **U6-1**, **Np6-1**, and **Pu6-1**) and C_i (right) (**Ce6-2**, **Th6-1**, **Th6-2**, **Th6-3**, **U6-2**, and **Pu6-2**) symmetries of the clusters.

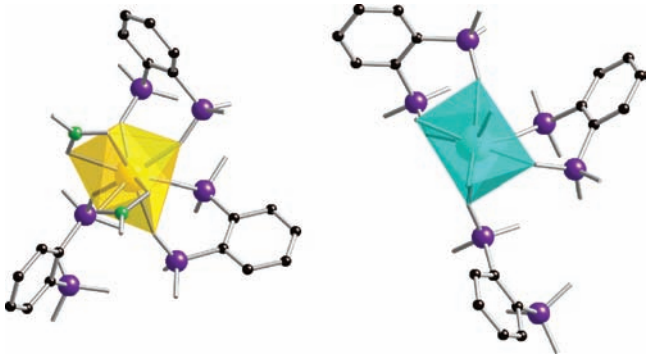

Figure 6. Views of the tricapped trigonal prism (PuO_9) and square antiprism (ThO_8) coordination environment.

The average bond distances for C_{3i} clusters of the same element are slightly larger than the C_i clusters.

The cavity size of clusters is tuned by the ionic radius of the +4 cation. For example, the largest cation, Th(IV), is selective for Cs^+ and Tl^+. Owing to the gap created by protactinium and the actinide contraction, U(IV) is considerably smaller than Th(IV), and we find that U(IV), Np(IV), and Pu(IV)/Ce(IV) all assemble around NH_4^+ or Rb^+ cations. As shown in Table 1, the distance to the center of the clusters is approximately 4.5 Å for the thorium clusters, but for all others it is ~4.4 Å, which is consistent with our comparison on average bond distances that Th^{4+} is much larger than the other ions. The cations that cocrystallize between clusters is also important for crystallization. In

dx.doi.org/10.1021/ic2023242 | Inorg. Chem. 2012, 51, 4088−4093

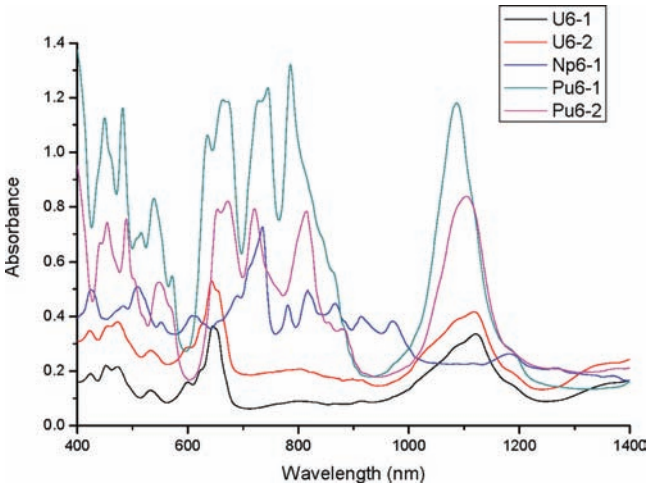

Figure 7. Vis-NIR absorption spectra of **U6-1** (black), **U6-2** (red), **Np6-1** (blue), **Pu6-1** (green), and **Pu6-2** (purple).

the U(IV) and Np(IV) clusters, both Rb^+ and Cs^+ cations were added to the reactions. However, only Rb^+ cations were found between the Np(IV) clusters, and only Cs^+ exists between the U(IV) clusters.

For all the C_{3i} clusters, there are always two NO_3^- groups bound to the metal centers. However, for the C_i clusters, the number of NO_3^- anions varies. For example, **Th6-1** has two NO_3^- anions bound to each Th(IV) center, whereas **Th6-2** has zero, one, or two NO_3^- groups around each cation. **Th6-3** has one NO_3^- anion that is disordered between two Th(IV) centers. The uranium cluster also can have different numbers of NO_3^- anions bound to the U(IV) cations. We also observed that nitrate can both chelate the metal centers and act as a bridge between metal centers as occurs in **Th6-3**. Ce(IV) and Pu(IV) have no measurable difference in ionic radius, and regardless of the crystal symmetry the metals are always bound by two NO_3^- groups. In **Th6-2** and **Th6-3**, there are unbound NO_3^- anions in the space between the clusters to balance the charge.

Absorption Spectroscopy. The UV−vis-NIR absorption spectra of **U6-1**, **U6-2**, **Np6-1**, **Pu6-1**, and **Pu6-2** were collected from single crystals using a microspectrophotometer. The spectra of cerium and thorium phases are not reported here because they lack f electrons. U(IV), Np(IV), and Pu(IV), which possess the electron configurations of $5f^2$, $5f^3$, and $5f^4$, respectively, are known to produce a series of weak, Laporte-forbidden f−f transitions in the vis-NIR. In most cases, these transitions show relatively small variations with changing coordination environments, and thus they can be used as fingerprints for a given oxidation state.[12]

For U(IV) in perchloric acid, the most intense f−f transitions are $^1D_2$ at 648 nm and $^3F_3$ at 1069 nm.[13] These two transitions can be also found in the spectra of both **U6-1** and **U6-2**. However, the $^1D_2$ transition is slightly blue-shifted to 642 nm, while the $^3F_3$ transition overlaps with $^3H_5$, producing a broadening peak at 1116 nm. Other transitions observed in solution such as $^1I_6$ (429 nm), $^8P_1$ (486 nm), $^8P_0$ (495 nm), and $^1G_4$ (549 nm) are all present in the spectra of both **U6-1** and **U6-2**. However, interestingly, all these transitions are blue-shifted to lower wavelength regions at 423, 452, 474, and 532 nm, respectively. The observation that the spectra for both **U6-1** and **U6-2** are principally the same is not surprising because the first coordination spheres for U(IV) centers in both compounds are very similar. Np(IV) in perchloric acid produces several intense transitions at approximately 730 nm (mixed transition), 960 nm ($^4I_{13/2}$), and 1150 nm ($^4F_{3/2}$).[14] In the spectrum of **Np6-1**, the mixed transition is still very intense at 734 nm, while the other two significantly weaker transitions are at 970 and 1182 nm, respectively. The spectrum of Pu(IV) in solution consists of a series of characteristic transitions such as the peaks near 477, 660, 800, and 1080 nm,[15] which can be all found in the spectra of **Pu6-1** and **Pu6-2**. Again, two Pu(IV) clusters produce spectra with only subtle differences.

CONCLUSIONS

Ten 4f/5f metal clusters have been prepared by self-assembly at room temperature. All are hexanuclear, but two different point groups for the clusters are observed that are not tied directly to periodic trends in the actinide series, such as the contraction across the row. Additional changes in the coordination environments of the metal centers, and counterions encapsulated within the clusters are found. The former differences are counterintuitive with the largest of the cations, Th(IV), exhibiting an eight-coordinate environment, whereas all of the smaller cations are exclusively found to be nine-coordinate. Clearfield's study on the uranyl phosphonate phase transformation showed that when exposed to moderate humidity, the uranyl phosphonate chain structure can transform from cis-α phase to trans-β phase. The α- and β- phase can further transform to the γ-phase, which is a uranyl nanotubular structure, with the existence of Na or Ca ions under aqueous conditions. Their kinetic studies indicate a mechanism of uranyl and phenylphosphonate disassembling followed by reassembling.[16] For the cluster systems, the X-ray scattering experiments on the uranium cluster suggest that these clusters assemble during crystallization and are likely not present in the initial reaction mixtures (Figure 1S, Supporting Information). While the metal phosphonate cores are likely quite stable, f-elements tend to show very fast ligand exchange kinetics.[17] The number of water molecules and nitrate anions bound to the exterior of the clusters is likely a function of subtle changes in crystallization conditions and is not a direct function of specific bonding aspects of a given An(IV) cation. We therefore suggest that the specific coordination number of the metal centers is difficult to control and immaterial for developing periodic trends in these clusters. In contrast, the size of the cavity in the clusters is a direct function of the ionic radius of the An(IV) cations. Th(IV) clusters form around Cs^+ or Tl^+ cations, whereas all of the other An(IV) cations assemble around smaller Rb^+ and/or NH_4^+ cations. Future work will develop larger clusters by changing the size and geometry of the bridging diphosphonate.

ASSOCIATED CONTENT

Supporting Information

Selected bond distances (Tables 1S−10S); SAXS data on U6 cluster (Figure 1S); crystallographic information files. This material is available free of charge via the Internet at http://pubs.acs.org.

AUTHOR INFORMATION

Corresponding Author

*E-mail: talbrec1@nd.edu.

Notes

The authors declare no competing financial interest.

dx.doi.org/10.1021/ic2023242 | Inorg. Chem. 2012, 51, 4088−4093

■ ACKNOWLEDGMENTS

We are grateful for support provided by the U.S. Department of Energy, Heavy Elements Chemistry Program, under Grant DE-SC0002215.

■ REFERENCES

(1) (a) Winpenny, R. E. P. *Chem. Soc. Rev.* **1998**, *27*, 447−452. (b) Lombardi, J. R.; Davis, B. *Chem. Rev.* **2002**, *102*, 2431−2460. (c) Long, D.-L.; Burkholder, E.; Cronin, L. *Chem. Soc. Rev.* **2007**, *36*, 105−121. (d) Dolbecq, A.; Dumas, E.; Mayer, C. R.; Mialane, P. *Chem. Rev.* **2010**, *110*, 6009−6048. (e) Seeber, G.; Tiedemann, B. E. F.; Raymond, K. N. *Top. Curr. Chem.* **2006**, *265*, 147−183.

(2) (a) Sigmon, G. E.; Burns, P. C. *J. Am. Chem. Soc.* **2011**, *133*, 9137−9139. (b) Ling, J.; Wallace, C. M.; Szymanowski, J. E. S.; Burns, P. C. *Angew. Chem., Int. Ed.* **2010**, *49*, 7271−7273. (c) Ling, J.; Qiu, J.; Sigmon, G. E.; Ward, M.; Szymanowski, J. E. S.; Burns, P. C. *J. Am. Chem. Soc.* **2010**, *132*, 13395−13402. (d) Sigmon, G. E.; Ling, J.; Unruh, D. K.; Moore-Shay, L.; Ward, M.; Weaver, B.; Burns, P. C. *J. Am. Chem. Soc.* **2009**, *131*, 16648−16649. (e) Sigmon, G. E.; Unruh, D. K.; Ling, J.; Weaver, B.; Ward, M.; Pressprich, L.; Simonetti, A.; Burns, P. C. *Angew. Chem., Int. Ed.* **2009**, *48*, 2737−2740. (f) Forbes, T. Z.; McAlpin, J. G.; Murphy, R.; Burns, P. C. *Angew. Chem., Int. Ed.* **2008**, *47*, 2824−2827.

(3) Cornet, S. M.; Haller, L. J. L.; Sarsfield, M. J.; Collison, D.; Helliwell, M.; May, I.; Kaltsoyannis, N. *Chem. Commun.* **2009**, 917−919.

(4) Soderholm, L.; Almond, P. M.; Skanthakumar, S.; Wilson, R. E.; Burns, P. C. *Angew. Chem., Int. Ed.* **2008**, *47*, 298−302.

(5) (a) Jerome, D. S.; Corbett, J. D. *J. Am. Chem. Soc.* **1984**, *106*, 4618−4619. (b) Ziebarth, R. P.; Corbett, J. D. *J. Am. Chem. Soc.* **1987**, *109*, 4844−4850. (c) Ziebarth, R. P.; Corbett, J. D. *J. Am. Chem. Soc.* **1985**, *107*, 4571−4573. (d) Hughbanks, T.; Rosenthal, G.; Corbett, J. D. *J. Am. Chem. Soc.* **1988**, *110*, 1511−1516. (e) Runyan, C. E.; Hughbanks, T.; Ziebarth, R. P.; Corbett, J. D. *J. Am. Chem. Soc.* **1994**, *116*, 7909−7910. (f) Zhong, W; Alexeev, D.; Harvey, I.; Guo, M.; Hunter, D. J. B.; Zhu, H.; Campopiano, D. J.; Sadler, P. J. *Angew. Chem., Int. Ed.* **2004**, *43*, 5914−5918. (g) Pan, L.; Heddy, R.; Li, J.; Huang, X.-Y.; Tang, X.; Kilpatrick, L. *Inorg. Chem.* **2008**, *47*, 5537−5539. (h) Das, R.; Sarma, R.; Baruah, J. B. *Inorg. Chem. Commun.* **2010**, *13*, 793−795. (i) Prasad, T. K.; Rajasekharan, V. *Inorg. Chem.* **2009**, *48*, 11543−11550. (j) Tasiopoulos, A. J.; O'Brien, T. A.; Abbound, K. A.; Christou, G. *Angew. Chem., Int. Ed.* **2004**, *43*, 345−349. (k) Yi, X.-Y.; Sung, H. H. Y.; Willliams, I. D.; Leung, W.-H. *Chem. Commun.* **2008**, 3269−3271. (l) Mereacre, V.; Ako, A. M.; Akhtar, M.; Lindemann, A.; Anson, C. E.; Powell, A. K. *Helv. Chim. Acta* **2009**, *92*, 2507−2524. (m) Tasiopoulos, A. J.; Milligan, P. L. Jr.; Annound, K. A.; O'Brien, T. A.; Christou, G. *Inorg. Chem.* **2007**, *46*, 9678−9691. (n) Mishra, A.; Abboud, K. A.; Christou, G. *Inorg. Chem.* **2006**, *45* (6), 2364−2366. (o) Mishra, A.; Tasiopoulos, A. J.; Wernsdorfer, W.; Abboud, K. A.; Christou, G. *Inorg. Chem.* **2007**, *46* (8), 3105−3115. (p) Tasiopoulos, A. J.; Mishra, A.; Christou, G. *Polyhedron* **2007**, *26* (9−11), 2183−2188. (q) Maayan, G.; Christou, G. *Inorg. Chem.* **2011**, *50* (15), 7015−7021.

(6) (a) Morky, L. M.; Dean, N. S.; Carrano, C. J. *Angew. Chem., Int. Ed.* **1996**, *35*, 1497−1498. (b) Takao, S.; Takao, K.; Kraus, W.; Emmerling, F.; Scheinost, A. C.; Bert, G.; Hennig, C. *Eur. J. Inorg. Chem.* **2009**, 4771−4775. (c) Berthet, J.-C.; Thuery, P.; Ephritikhine, M. *Chem. Commun.* **2005**, 3415−3417. (d) Mougel, V.; Biswas, B.; Pecaut, J.; Mazanti, M. *Chem. Commun.* **2010**, *46*, 8648−8650. (e) Berthet, J.-C.; Thuery, P.; Ephritikhine, M. *Inorg. Chem.* **2010**, *49*, 8173−8177. (f) Duval, P. B.; Burns, C. J.; Clark, D. L.; Morris, D. E.; Scott, B. L.; Thompson, J. D.; Werkema, E. L.; Jia, L.; Anderson, R. A. *Angew. Chem., Int. Ed.* **2001**, *40*, 3357−3361. (g) Nocton, G.; Burdet, F.; Pecaut, J.; Mazzanti, M. *Angew. Chem., Int. Ed.* **2007**, *46*, 7574−7578. (h) Nocton, G.; Pecaut, J.; Filinchuk, Y.; Mazzanti, M. *Chem. Commun.* **2010**, *46*, 2757−2759.

(7) Knope, K. E.; Wilson, R. E.; Vasiliu, M.; Dixon, D. A.; Soderholm, L. *Inorg. Chem.* **2011**, *50*, 9696−9704.

(8) Diwu, J.; Good, J. J.; DiStefano, V. H.; Albrecht-Schmitt, T. E. *Eur. J. Inorg. Chem.* **2011**, 1374−1377.

(9) (a) Sheldrick, G. M. *SHELXTL PC*, Version 5.0; Siemens Analytical X-Ray Instruments, Inc.: Madison, WI, 1994; (b) Sheldrick, G. M. *SADABS, Program for Absorption Correction Using SMART CCD Based on the Method of Blessing*; Blessing, R. H. *Acta Crystallogr.* **1995**, *A51*, 33-38.

(10) Clark, D. L.; Hecker, S. S.; Jarvinen, G. D.; Neu, M. P. Plutonium. In *The Chemistry of the Actinide and Transactinide Elements*; Morss, L. R.; Edelstein, N. M.; Fuger, J., Eds.; Springer: The Netherlands, 2006; Vol. *2*, Chapter 7, pp 1110−1113;

(11) Gorden, A. E. V; Xu, J.; Raymond, K. N.; Durbin, P. *Chem. Rev.* **2003**, *103*, 4207−4282.

(12) (a) Liu, G.; Beitz, J. V. Spectra and Electronic Structures of Free Actinide Atoms. In *The Chemistry of the Actinide and Transactinide Elements*; Morss, L. R.; Edelstein, N. M.; Fuger, J., Eds.; Springer: The Netherlands, 2006; Vol. *4*, Chapter 16, pp 2013−2111; (b) Carnall, W. T.; Liu, G. K.; Williams, C. W.; Reid, M. F. *J. Chem. Phys.* **1991**, *95*, 7194−7203.

(13) Cohen, D.; Carnall, W. T. *J. Phys. Chem.* **1960**, *64*, 1933−1936.

(14) Hagan, P. G.; Cleveland, J. M. *J. Inorg. Nucl. Chem.* **1966**, *28*, 2905−2909.

(15) (a) Cohen, D. *J. lnorg. Nucl. Chem.* **1961**, *18*, 211−218. (b) Lee, M. H.; Park, Y. J.; Kim, W. H. *J. Radioanal. Nucleic Chem.* **2007**, *273*, 375−382.

(16) Grohol, D.; Clearfield, A. *J. Am. Chem. Soc.* **1997**, *119*, 9301−9302.

(17) (a) Helm, L.; Merbach, A. E. *Chem. Rev.* **2005**, *105*, 1923−1959. (b) Szabo, Z.; Toraishi, T.; Vallet, V.; Grenthe, I. *Coord. Chem. Rev.* **2006**, *250*, 784−815.